

# Engineered Hyperphosphorylation of the $\beta_2$ -Adrenoceptor Prolongs Arrestin-3 Binding and Induces Arrestin Internalization

Diana Zindel, Adrian J. Butcher, Suleiman Al-Sabah, Peter Lanzerstorfer, Julian Weghuber, Andrew B. Tobin, Moritz Bünemann, and Cornelius Krasel

*Institut für Pharmakologie und Klinische Pharmazie, Philipps-Universität Marburg, Marburg, Germany (D.Z., M.B., C.K.); MRC Toxicology Unit, University of Leicester, Leicester, United Kingdom (A.J.B., A.B.T.); Department of Pharmacology and Toxicology, Kuwait University, Kuwait (S.A.-S.); and University of Applied Sciences Upper Austria, Wels, Austria (P.L., J.W.)*

Received August 13, 2014; accepted November 24, 2014

## ABSTRACT

G protein-coupled receptor phosphorylation plays a major role in receptor desensitization and arrestin binding. It is, however, unclear how distinct receptor phosphorylation patterns may influence arrestin binding and subsequent trafficking. Here we engineer phosphorylation sites into the C-terminal tail of the  $\beta_2$ -adrenoceptor ( $\beta_2$ AR) and demonstrate that this mutant, termed  $\beta_2$ AR<sup>SSS</sup>, showed increased isoprenaline-stimulated phosphorylation and differences in arrestin-3 affinity and trafficking. By measuring arrestin-3 recruitment and the stability of arrestin-3 receptor complexes in real time using fluorescence resonance energy transfer and fluorescence recovery after photobleaching, we demonstrate that arrestin-3 dissociated quickly and almost completely from the  $\beta_2$ AR, whereas the interaction with  $\beta_2$ AR<sup>SSS</sup> was 2- to 4-fold prolonged. In contrast, arrestin-3 interaction

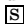
with a  $\beta_2$ -adrenoceptor fused to the carboxyl-terminal tail of the vasopressin type 2 receptor was nearly irreversible. Further analysis of arrestin-3 localization revealed that by engineering phosphorylation sites into the  $\beta_2$ -adrenoceptor the receptor showed prolonged interaction with arrestin-3 and colocalization with arrestin in endosomes after internalization. This is in contrast to the wild-type receptor that interacts transiently with arrestin-3 at the plasma membrane. Furthermore,  $\beta_2$ AR<sup>SSS</sup> internalized more efficiently than the wild-type receptor, whereas recycling was very similar for both receptors. Thus, we show how the interaction between arrestins and receptors can be increased with minimal receptor modification and that relatively modest increases in receptor-arrestin affinity are sufficient to alter arrestin trafficking.

## Introduction

Arrestins are a small family of four homologous proteins that have evolved as multifunctional scaffolding and adaptor proteins in G protein-coupled receptor (GPCR) signaling and trafficking. High-affinity arrestin interaction with GPCRs is mediated by a two-step process that involves receptor activation and phosphorylation in a synergistic fashion. Phosphorylation of agonist activated receptors is catalyzed by G protein-coupled receptor kinases (GRKs), of which seven different isoforms have been identified (Pitcher et al., 1998). Almost all GPCRs are phosphorylated by one or more of the seven GRKs, which are, in addition to arrestin binding, receptor desensitization, and uncoupling of G proteins, considered to regulate cell type-specific receptor signaling (Tobin

et al., 2008). For rhodopsin it has been shown that the extent of arrestin receptor interaction varies in a systematic manner with the number of residues that are phosphorylated (Vishnivetskiy et al., 2007). In the  $\beta_2$ AR the three serine residues S355, S356, and S364 have a pivotal role in GRK-mediated phosphorylation and desensitization (Seibold et al., 2000; Vaughan et al., 2006) as well as arrestin binding (Krasel et al., 2008). The recently developed “bar code” hypothesis postulates that site-specific phosphorylation of GPCRs may regulate specific signaling outcomes (Tobin et al., 2008). Studies that support this hypothesis have been published recently for the  $\beta_2$ -adrenoceptor (Nobles et al., 2011), muscarinic acetylcholine receptor M<sub>3</sub> (Butcher et al., 2011), CCR7 (Zidar et al., 2009), and the vasopressin type 2 receptor (V2R) (Ren et al., 2005). On the other hand, for the activity of rhodopsin it has been shown that receptor activity depends solely on the number but not on the identity of phosphorylation sites (Doan et al., 2006). Based on the apparent stability of arrestin-receptor complexes, GPCRs have been divided into two classes, A and B (Oakley et al., 2000). Class A receptors such as the  $\beta_2$ -adrenoceptor,  $\mu$ -opioid receptor, or endothelin type A receptor recruit preferentially arrestin-3 and show a transient arrestin interaction primarily at the plasma membrane.

This work was supported by the Deutsche Forschungsgemeinschaft as part of the project A13 of the SFB593 “Mechanisms of cellular compartmentalisation and the relevance for disease.” Part of this work was supported by a BBSRC new investigator grant to C.K. [Grant BB/D012902/1]. D.Z. was the recipient of a DAAD PROMOS Travel Grant. A.J.B. and A.B.T. are funded by a MRC program leader grant through the MRC Toxicology Unit.  
dx.doi.org/10.1124/mol.114.095422.

 This article has supplemental material available at molpharm.aspetjournals.org.

**ABBREVIATIONS:**  $\beta_2$ AR,  $\beta_2$ -adrenoceptor; CFP, cyan fluorescent protein; CGP12,177, 4-[3-[(1,1-dimethylethyl)amino]2-hydroxypropoxy]-1,3-dihydro-2H-benzimidazol-2-one; FRAP, fluorescence recovery after photobleaching; FRET, fluorescence resonance energy transfer; GPCR, G protein-coupled receptor; GRK, G protein-coupled receptor kinase; KT 5720, (9R,10S,12S)-2,3,9,10,11,12-hexahydro-10-hydroxy-9-methyl-1-oxo-9,12-epoxy-1H-diolindolo [1,2,3-fg:3',2',1'-k]pyrrolo[3,4-j][1,6]benzo-diazocine-10-carboxylic acid hexyl ester; PKA, protein kinase A; YFP, yellow fluorescent protein.

In contrast, class B receptors, e.g., the V2R or the angiotensin II type 1A receptor, bind both arrestin-2 and arrestin-3 with similar high affinities and colocalize with them on endosomes (Oakley et al., 2000). The swapping of the C termini of  $\beta_2$ -adrenoceptor and V2R was found to reverse the trafficking pattern and signaling properties of arrestin (Oakley et al., 2000, 2001; Tohgo et al., 2003). Recently, a similar phenomenon was described for the switch of the C termini of the NK1R and PAR<sub>2</sub> (Pal et al., 2013). In both cases, clusters of Ser and Thr residues localized approximately 20–30 amino acids away from the membrane were proposed to be the major binding sites for arrestins. It was suggested that clusters of phosphorylated residues would increase the affinity of arrestin for the receptor. However, these findings were obtained by swapping the entire C termini of different receptors. It is known that receptor C termini possess additional functions in addition to arrestin binding. For example, the C terminus of the  $\beta_2$ AR provides binding sites for adaptor proteins like Grb2 (Karoor et al., 1998) and PDZ-binding proteins like NHERF (Hall et al., 1998), which promotes rapid recycling of the receptor after agonist-induced internalization (Cao et al., 1999). In this study we investigate whether the insertion of an additional cluster of serines into the C terminus of the  $\beta_2$ AR 20 amino acids away from the membrane, as previously proposed by Oakley et al. (2001), can indeed enhance arrestin binding affinity to the receptor and alter arrestin trafficking without affecting other properties such as receptor recycling.

## Materials and Methods

Unless otherwise stated, all biochemicals and reagents were from Sigma (Taufkirchen, Germany).

**DNA Constructs and Transient Expression in HEK 293T Cells or Stable Expression in HEK 293 Cells.** The following constructs have been described elsewhere: the  $\beta_2$ V2R in which the C-terminal tail has been replaced with the V2R-tail (Oakley et al., 1999), the phosphorylation-deficient  $\beta_2$ AR ( $\beta_2$ AR<sup>pd</sup>) lacking all putative phosphorylation sites except for the protein kinase A (PKA) phospho-sites (Bouvier et al., 1988), arrestin-3–cyan fluorescent protein (CFP) (Krasel et al., 2005), GRK2 (Krasel et al., 2001), G $\beta$ 1-Cer (Frank et al., 2005), G $\alpha_s$  (Hein et al., 2006), and G $\gamma_2$  (Lutz et al., 2005). Mutations were inserted into the  $\beta_2$ AR by site-directed mutagenesis. The  $\beta_2$ AR<sup>SSS</sup> was generated by replacing G-361, E-362, and Q-363 of the yellow fluorescent protein (YFP)–labeled or the unlabeled, N-terminally Flag-tagged receptor with serine residues. The  $\beta_2$ AR<sup>AAA</sup> was constructed by replacing G-361, E-362, and Q-363 of the YFP-labeled or the unlabeled receptor with alanine residues.  $\beta_2$ AR 2S was generated by reintroducing Ser 355/356 into the  $\beta_2$ AR<sup>pd</sup> construct.  $\beta_2$ AR 3S was constructed by replacing G-361, E-362, and Q-363 of the  $\beta_2$ AR<sup>pd</sup> construct with serine residues, and the  $\beta_2$ AR 5S construct was produced by applying both steps successively.  $\beta_2$ AR SSS distal was generated by replacing N-398, I-399, and D-400 with serines. The amino acid sequences encoded by the different receptor constructs are shown in Fig. 1. Receptor constructs that were used for the fluorescence recovery after photobleaching (FRAP) assay were N-terminally tagged with YFP (Dorsch et al., 2009). mCherry-tagged EEA1 was constructed by replacing the GFP in EEA1-GFP (a gift from Nicholas Holliday and Simon Davies, University of Nottingham, UK) with mCherry. All cDNAs were cloned into the pcDNA3 expression vector (Invitrogen, Darmstadt, Germany) and verified by sequencing. HEK 293T cells were maintained in Dulbecco's modified Eagle's medium supplemented with 10% fetal calf serum, penicillin (50  $\mu$ g/ml), and streptomycin (50  $\mu$ g/ml). Stable and transient transfections were performed using Effectene (Qiagen, Hilden, Germany) following the manufacturer's protocol.

**Receptor Expression Levels.** HEK293 cells stably expressing Flag- $\beta_2$ AR, Flag- $\beta_2$ AR<sup>SSS</sup>, or  $\beta_2$ AR<sup>AAA</sup> were generated by standard procedures using G418 (600  $\mu$ g/ml) selection. To determine receptor

expression levels in membranes from these cells, confluent grown cells were washed in ice-cold phosphate-buffered saline and detached with buffer composed of 50 mM NaCl, 20 mM NaH<sub>2</sub>PO<sub>4</sub>, 3 mM MgCl<sub>2</sub>, 1 mM EDTA, pH 7.4, containing protease inhibitor cocktail from Roche (Penzberg, Germany; 1 tablet per 10 ml). Membranes were pelleted by centrifugation at 14,000 rpm for 1 hour at 4°C. The pellet was washed in 100 mM NaCl, 20 mM Tris, pH 7.4, resuspended in the same buffer and subsequently sonified. Membrane receptor binding was measured using saturating concentrations of [<sup>3</sup>H]dihydroalprenolol. Nonspecific binding was measured in the presence of 100  $\mu$ M alprenolol. Binding was performed overnight at 4°C, and bound and unbound ligand were separated on GF/C glass fiber filters (Whatman, Dassel, Germany) by vacuum filtration. Filters were washed four times with 4 ml ice-cold buffer (50 mM Tris HCl, 120 mM NaCl, pH 7.4) and counted using a liquid scintillation  $\beta$ -counter (Packard 1600 TR). The expression of Flag- $\beta_2$ AR, Flag- $\beta_2$ AR<sup>SSS</sup>, or Flag- $\beta_2$ AR<sup>AAA</sup> was 64, 80, and 79 pmol/mg membrane protein, respectively. Expression levels of transiently transfected cells were ranging from 15 to 50 pmol/mg membrane protein.

**[<sup>32</sup>P]Orthophosphate Labeling and  $\beta_2$ AR Immunoprecipitation.** [<sup>32</sup>P]Orthophosphate labeling, agonist incubation, receptor solubilization, immunoprecipitation, and autoradiography were done as described previously (Butcher et al., 2011). Briefly, HEK 293 cells stably expressing Flag- $\beta_2$ -adrenoceptors were grown in six well plates. After washing and incubation with KH<sub>2</sub>PO<sub>4</sub>-free KREBS buffer (118.4 mM NaCl, 4.7 mM KCl, 4.2 mM NaHCO<sub>3</sub>, 1.2 mM MgSO<sub>4</sub>, 11.7 mM glucose, 10 mM HEPES, pH 7.4) containing 100  $\mu$ Ci/ml [<sup>32</sup>P]orthophosphate (Perkin Elmer, Billerica, MA), cells were stimulated for 5 minutes with 10  $\mu$ M isoprenaline. Cells were then lysed immediately (20 mM Tris, 150 mM NaCl, 3 mM EDTA, 1% IGEPAL-CA-630, pH 7.4) and immunoprecipitated using anti-Flag-M2 affinity gel. Immunoprecipitated proteins were resolved using gel electrophoresis on 8% SDS gels and visualized by autoradiography. Part of the immunoprecipitated proteins was transferred onto a polyvinylidene fluoride membrane and subsequently immunoblotted with a polyclonal anti-Flag antibody for the detection of total receptors.

**Microscopic Fluorescence Resonance Energy Transfer Measurements and Data Evaluation.** Dynamics of G protein receptor interaction or arrestin-receptor interaction, respectively, were performed as previously reported (Krasel et al., 2005; Bodmann et al., 2014). In brief, 24 hours after transfection cells were split on poly-lysine-coated 25 mm coverslips and, after an additional 14–16 hours, were analyzed by fluorescence resonance energy transfer (FRET) microscopy using an inverted eclipse Ti Nikon microscope. Cells were maintained and continuously superfused in either FRET buffer (137 mM NaCl, 5.4 mM KCl, 2 mM CaCl<sub>2</sub>, 1 mM MgCl<sub>2</sub>, and 10 mM HEPES, pH 7.3) or 1  $\mu$ M isoprenaline in FRET buffer at room temperature using a fast switching perfusion system (Ala-VC3-8SP; ALA Scientific Instruments, Farmingdale, NY). Cells were observed using a 100 $\times$  oil immersion objective (Plan Apo VC 100 $\times$ /1.40 NA oil; Nikon, Düsseldorf, Germany). CFP was excited with 435 nm light using an excitation filter 430/24 and a beam splitter T455LP. All filters were from Chroma (Olching, Germany). The light source was a Lambda DG4 (Sutter, Novato, CA). Some experiments were performed with an LED excitation system (pE-2, CoolLED, Andover, UK). Fluorescence emission from CFP (F<sub>480</sub>) and YFP (F<sub>535</sub>) were collected using a beam splitter CFP/YFP (z 488/800-1064 rpc), emission filter F<sub>480</sub> (480/40), and emission filter F<sub>535</sub> (535/30). The illumination frequency was set to 2.5 Hz and illumination time was set to 30–40 milliseconds to minimize photobleaching. A charge-coupled device camera (Evolve 512; Photometrics, Tucson, AZ) was used to detect the signals; FRET was calculated as F<sub>YFP</sub>/F<sub>CFP</sub>. Spillover of CFP into the YFP channel was corrected, whereas direct YFP excitation was negligible. Individual FRET recordings were averaged and are either shown as absolute alterations in FRET normalized to the baseline or normalized to the individual agonist-induced response as a maximum and to the baseline as minimum, to display the kinetics. The dissociation and association kinetics in the presence of overexpressed GRK2 were fitted using the following monoexponential equations: dissociation:  $y(t) = A \times (e^{-k_{off} \times t}) + y_0$ ; association:  $y(t) = A \times (1 - e^{-k_{on} \times t}) + y_0$ .

human $\beta$ 2AR	F <sub>336</sub> QELLCLRRSSLKAYGNGYSSNGTGEQSGYHVEQEKENKLLCEDLPGTEDFVGHQGTVPDNDISQGRNCSTNDSL
$\beta$ 2AR SSS	F <sub>336</sub> QELLCLRRSSLKAYGNGYSSNGT <b>SSSS</b> SGYHVEQEKENKLLCEDLPGTEDFVGHQGTVPDNDISQGRNCSTNDSL
$\beta$ 2AR AAA	F <sub>336</sub> QELLCLRRSSLKAYGNGYSSNGT <b>AAAS</b> SGYHVEQEKENKLLCEDLPGTEDFVGHQGTVPDNDISQGRNCSTNDSL
$\beta$ 2AR pd	F <sub>336</sub> QELLCLRRSSLKAYGNGY <b>AG</b> NGN <b>AGE</b> QGGYHVEQEKENKLLCEDLPG <b>AED</b> DFVGHQ <b>GAV</b> PGDNID <b>AQ</b> GRNC <b>GAND</b> ALL
$\beta$ 2AR 2S	F <sub>336</sub> QELLCLRRSSLKAYGNGYSSNGN <b>AGE</b> QGGYHVEQEKENKLLCEDLPG <b>AED</b> DFVGHQ <b>GAV</b> PGDNID <b>AQ</b> GRNC <b>GAND</b> ALL
$\beta$ 2AR 3S	F <sub>336</sub> QELLCLRRSSLKAYGNGY <b>AG</b> NGN <b>ASS</b> SGYHVEQEKENKLLCEDLPG <b>AED</b> DFVGHQ <b>GAV</b> PGDNID <b>AQ</b> GRNC <b>GAND</b> ALL
$\beta$ 2AR 5S	F <sub>336</sub> QELLCLRRSSLKAYGNGYSSNGN <b>ASS</b> SGYHVEQEKENKLLCEDLPG <b>AED</b> DFVGHQ <b>GAV</b> PGDNID <b>AQ</b> GRNC <b>GAND</b> ALL
$\beta$ 2AR SSS distal	F <sub>336</sub> QELLCLRRSSLKAYGNGYSSNGTGEQSGYHVEQEKENKLLCEDLPGTEDFVGHQGTVPD <b>SSSS</b> SQGRNCSTNDSL
$\beta$ 2V2	F <sub>336</sub> QELL <b>CARGRTPPSLGPQDESC</b> T <b>TASSSLAKDTSS</b>

**Fig. 1.** Sequence alignment of the human  $\beta$ 2AR variants used in this study. Shown are all residues of the  $\beta$ 2AR starting at phenylalanine 336, which is located at the beginning of the intracellular C-terminal tail. Amino acids used for replacement are underlined and highlighted in the corresponding mutant sequences in bold. In the  $\beta$ 2V2R the entire C terminus of the  $\beta$ 2AR was replaced by the C terminus of the vasopressin 2 receptor.

Concentration-response curves for receptor-G protein interaction were obtained by measuring amplitudes of FRET changes.

**Quantification of Relative Expression Levels.** In experiments in which FRET amplitudes are shown, relative expression levels of fluorescently labeled proteins were determined as described before (Wolters et al., 2015). In brief, both fluorophores were excited individually and background fluorescence was subtracted for each channel. The calibration factor of a reference construct YFP- $\beta$ 2AR-CFP (Dorsch et al., 2009) was calculated as  $F_{YFP}/F_{CFP}$ . For each individual FRAP recording, the factor  $F_{YFP}/F_{CFP}$  was calculated the same way.

**Dual Color FRAP Microscopy.** A protocol for arrestin-3 mobility at the plasma membrane was established based on a method that had been developed earlier in our laboratory (Dorsch et al., 2009). HEK 293T cells transiently expressing arrestin-3-CFP and N-terminally YFP-tagged receptors grown on coverslips were washed in BE buffer (150 mM NaCl, 2.5 mM KCl, 10 mM HEPES, 12 mM glucose, 0.5 mM CaCl<sub>2</sub> and 0.5 mM MgCl<sub>2</sub>, pH 7.5) (Digby et al., 2006) followed by crosslinking N-terminally labeled receptors for 30 minutes at 37°C using a polyclonal GFP antibody (Rockland, Gilbertsville, PA) diluted 1:100 and supplemented with 2.5% fatty acid-free bovine serum albumin. Subsequently cells were washed three times in BE buffer and maintained in the same buffer containing 10  $\mu$ M isoprenaline for imaging purposes. FRAP microscopy was performed at 20°C using a Leica TCS SP5 scanning confocal microscope (Leica, Wetzlar, Germany) with a Lambda Blue 63 $\times$ /1.4 NA oil-immersion objective. CFP was excited at 405 nm with a diode laser, and CFP emission was collected at 450–489 nm. YFP was excited at 514 nm using an argon ion laser, and YFP emission was collected at 525–600 nm. The scan speed was set to 400 Hz, image format was 512  $\times$  512 pixels, the zoom factor was set to 6.0, and the pinhole was set to airy 1. During bleaching in the equatorial plane of the cell membrane, laser intensity was set to 70% to achieve 60–80% loss of fluorescence in a 3  $\times$  1  $\mu$ m rectangular area. Fluorescence recovery into the bleached membrane segment was monitored for 3–5 minutes at low laser intensity of 10%. Pixel intensities for CFP and YFP, respectively, were corrected for bleaching and CFP bleed through into the YFP channel. The lowest intensity directly after bleaching was subtracted from all other intensities after bleaching. Resulting FRAP curves were averaged, plotted as mean  $\pm$  S.E., and fitted with GraphPad Prism 4 (GraphPad Software, San Diego, CA) using a two phase association:  $Y = Y_0 + \text{Span}_{\text{Fast}} * (1 - \exp^{-k_{\text{Fast}} * X}) + \text{Span}_{\text{Slow}} * (1 - \exp^{-k_{\text{Slow}} * X})$ .

**$\mu$ -Patterning and Total Internal Reflection Fluorescence Microscopy.**  $\mu$ -Contact printing was performed as reported previously (Lanzerstorfer et al., 2014). The detection system was set up on an epifluorescence microscope (Olympus IX81; Olympus, Munich, Germany). Diode lasers (Toptica Photonics, Munich, Germany) were used for selective fluorescence excitation of CFP, YFP, and Cy5 at 405, 515, and 640 nm, respectively. The 405 nm diode laser (Toptica Photonics) was used for bleaching of YFP fluorescence (arrestin-3). Samples were illuminated in total internal reflection configuration (CellTIRF; Olympus) using a 60 $\times$  oil immersion objective (NA = 1.49, APON 60XO TIRF; Olympus). After appropriate filtering using

standard filter sets, fluorescence was imaged onto a charge-coupled device camera (Orca-R2; Hamamatsu, Japan). Samples were mounted on an x-y-stage (CMR-STG-MHIX2-motorized table; Märzhäuser, Germany), and scanning of larger areas was supported by a laser-guided automated focus-hold system (ZDC-2; Olympus). For FRAP experiments, single patterns were photobleached with a laser pulse (405 nm) applied for 600 milliseconds. Recovery images were recorded at indicated time intervals. FRAP images were analyzed using the Spotty framework (Borgmann et al., 2012). Data were normalized by the pre-bleach image, and curve fitting was done using Graphpad Prism. Resulting FRAP curves were plotted based on the standard error of the mean (S.E.) and fitted using a biexponential equation. Kinetic FRAP parameters were directly obtained from curve fitting.

**Confocal Microscopy.** HEK293T cells grown on 6 cm dishes were transiently transfected with labeled or unlabeled Flag- $\beta$ 2AR, Flag- $\beta$ 2AR<sup>SSS</sup>, or Flag- $\beta$ 2V2R, along with arrestin-3-CFP, GRK2, and mCherry-EEA1. Twenty-four hours posttransfection, cells were plated on 25 mm coverslips. Cells were either unstimulated or stimulated with 10  $\mu$ M isoprenaline for 30 minutes at 37°C and then fixed with 4% paraformaldehyde. Cells expressing fluorescent proteins were examined for arrestin localization and colocalization with EEA1. Confocal images were obtained on a Leica TCS SP5 scanning confocal microscope with a Lambda Blue 63 $\times$ /1.4 NA oil-immersion objective. CFP was excited at 405 nm with a diode laser, and CFP emission was collected at 452–543 nm. mCherry was excited at 543 nm using an HeNe laser; mCherry-emission was collected at 610–674 nm. YFP was excited at 514 nm; YFP emission was collected at 525–600 nm.

**Image Analysis.** To measure the dependency of pixels in dual channel images we used ImageJ 1.47 (<http://imagej.nih.gov/ij/>) and a colocalization plugin. Images for each channel were background subtracted and Pearson's colocalization coefficient was calculated using the following equation:

$$R_p = \frac{\sum(A_i - a) \times (B_i - b)}{\sqrt{[\sum(A_i - a)^2 \times \sum(B_i - b)^2]}}$$

The channel A and channel B gray values of voxel  $i$  are noted as  $A_i$  and  $B_i$ , respectively, and the average intensities over the full image as  $a$  and  $b$ .

**Receptor Internalization and Recycling.** Receptor internalization and recycling were quantified using [<sup>3</sup>H]CGP12,177 (4-[3-[(1,1-dimethylethyl)amino]2-hydroxypropoxy]-1,3-dihydro-2H-benzimidazol-2-one) (Hartmann Analytic, Braunschweig, Germany) binding. HEK293T cells transiently transfected with either Flag- $\beta$ 2AR or Flag- $\beta$ 2AR<sup>SSS</sup> were treated for 30 minutes at 37°C with 1  $\mu$ M isoprenaline in FRET buffer containing 10 mM glucose. The cells were then chilled on ice to stop membrane trafficking and were washed for four times with ice-cold FRET buffer containing 10 mM glucose to remove the isoprenaline. Afterward, they were allowed to recycle internalized receptor for various times at 37°C. At the end of the recycling period, cells were put on ice again and cell surface receptor was quantified by [<sup>3</sup>H]CGP12,177 binding as described (Krasel et al., 2005). Background binding was determined in the presence of 1  $\mu$ M alprenolol.

## Results

**Agonist-Induced Receptor Phosphorylation.** In the current study, we introduced three serine residues into the C terminus of the  $\beta$ 2AR 20 residues downstream from the palmitoylated Cys341 ( $\beta$ 2AR<sup>SSS</sup>) in analogy to the V2 vasopressin receptor that possesses a similar Ser cluster at exactly the same distance from its putative palmitoylation site (Fig. 1). It was anticipated that these residues might provide additional phosphorylation sites to those already present in this region of the receptor that would also serve to increase arrestin binding to the phosphorylated receptor (Fig. 1). The phosphorylation status of this mutant receptor and that of the wild-type receptor and a control construct where alanine residues were introduced ( $\beta$ 2AR<sup>AAA</sup>) was determined by <sup>32</sup>P metabolic labeling followed by receptor immunoprecipitation. All constructs tested showed low basal phosphorylation, which was robustly increased upon stimulation with 10  $\mu$ M isoprenaline for 5 minutes (Fig. 2A). After quantitation using densitometry, a substantial increase in receptor phosphorylation for  $\beta$ 2AR<sup>SSS</sup> was observed compared with  $\beta$ 2AR (Fig. 2B), suggesting that the additional serine residues are phosphorylated in an agonist-dependent manner, a conclusion supported by the fact that phosphorylation of the  $\beta$ 2AR<sup>AAA</sup> construct appeared similar to that of the wild-type  $\beta$ 2AR.

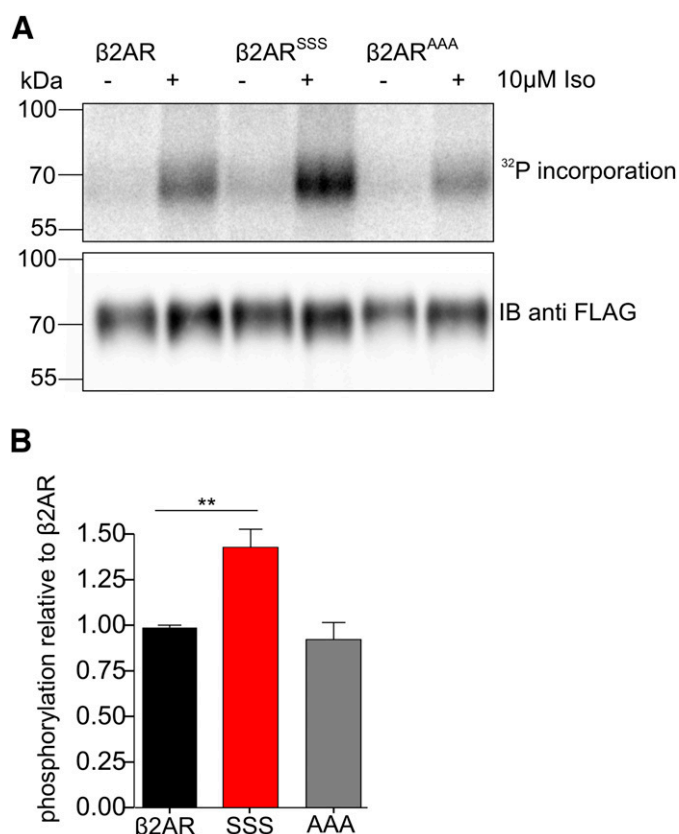


**Fig. 2.** <sup>32</sup>P incorporation after isoprenaline treatment. (A) HEK 293 cells stably expressing either Flag- $\beta$ 2AR, Flag- $\beta$ 2AR<sup>SSS</sup>, or Flag- $\beta$ 2AR<sup>AAA</sup> were immunoprecipitated and phosphorylated proteins identified by autoradiography (upper panel); equal receptor expression was confirmed by Western blotting (lower panel). (B) Quantification of agonist-induced phosphorylation as presented in (A). Results are mean  $\pm$  S.E. of 3–5 independent experiments \*\* $P < 0.01$ , one-way analysis of variance followed by Dunnett's multiple comparison test.

**G<sub>s</sub> Protein Coupling.** To investigate whether the introduction of the three serine residues would alter the coupling of the  $\beta$ 2AR to G<sub>s</sub> protein, a FRET-based assay was used to evaluate the interaction between the receptor and the G $\beta\gamma$  subunit of the heterotrimeric G<sub>s</sub> protein upon receptor activation (Hein et al., 2006). In these experiments HEK293T cells transiently transfected with various  $\beta$ 2ARs and the three G<sub>s</sub> subunits were superfused with isoprenaline at concentrations ranging from 100 pM to 10  $\mu$ M (Fig. 3A). In this assay, levels of receptor and G<sub>s</sub> are increased and most probably in excess of endogenous arrestin, therefore little receptor desensitization is expected. The wild-type  $\beta$ 2AR showed G<sub>s</sub> protein activation with an EC<sub>50</sub> value of 9.8 nM (Fig. 3B). A mutant receptor in which 12 phosphorylation sites had been mutated to alanine or glycine to generate a receptor that was significantly reduced in agonist-mediated phosphorylation ( $\beta$ 2AR<sup>pd</sup>; see Fig. 1 for sequence) (Bouvier et al., 1988) showed activation of G<sub>s</sub> protein that was not significantly different from the wild-type receptor (EC<sub>50</sub> = 7.7 nM) (Fig. 3B). G<sub>s</sub> protein activation via the  $\beta$ 2AR<sup>SSS</sup> mutant receptor occurred at slightly higher agonist concentrations but was not significantly different from the wild-type receptor (EC<sub>50</sub> = 25.8 nM) (Fig. 3B). These data indicate that G protein coupling is not adversely affected in the  $\beta$ 2AR<sup>SSS</sup> mutant.

**Receptor Phosphorylation and Interaction with Arrestin.**  $\beta$ -Adrenoceptors recruit arrestins in a phosphorylation-dependent manner. The removal of phospho-acceptor sites within the proximal C-terminal tail of the  $\beta$ 2AR leads to a marked attenuation of arrestin-3 binding, whereas the more distal phosphorylation sites in the C-terminal tail do not influence the affinity of arrestin-3 for the receptor (Seibold et al., 1998; Krasel et al., 2008). To monitor the association and dissociation kinetics of arrestin-receptor interaction, we used a FRET-based assay employing arrestin-3 and  $\beta$ 2AR tagged with YFP and CFP, respectively (Krasel et al., 2005). The association constant for  $\beta$ 2AR<sup>AAA</sup> was slowed significantly compared with  $\beta$ 2AR and the  $\beta$ 2AR<sup>SSS</sup> (Fig. 4A; Table 1). More importantly, the off-rate of the  $\beta$ 2AR was significantly reduced in the  $\beta$ 2AR<sup>SSS</sup> mutant (Fig. 4, A and B; Table 1). Furthermore, whereas arrestin-3 almost completely dissociated from the wild-type receptor during the time course of the experiment, dissociation of arrestin-3 from the  $\beta$ 2AR<sup>SSS</sup> was significantly reduced (Fig. 4A; Table 1). In contrast, arrestin-3 interaction with  $\beta$ 2V2R was nearly irreversible as only a small portion of the previously bound arrestin-3 actually dissociated on the timescale of the experiment (Fig. 4A; Table 1). However, the fraction of arrestin-3 that dissociated from the  $\beta$ 2V2R did so with faster kinetics compared with  $\beta$ 2AR<sup>SSS</sup> (Fig. 4, A and B; Table 1). Importantly, the off-rate of the  $\beta$ 2AR<sup>AAA</sup> was similar to that of the wild-type  $\beta$ 2AR (Fig. 4, A and B; Table 1). Hence, it appeared that the introduction of phosphorylation sites into the  $\beta$ 2AR increased its affinity for arrestin-3 as shown by a decrease in the rate and extent of dissociation.

The data above were measured in the presence of overexpressed GRK2. We also tested whether the observed differences arrestin-3 dissociation kinetics were still present with endogenous GRK levels. In cells not transfected with GRK2, the rate of arrestin-3 dissociation from the wild-type receptor was not significantly different from that of cells overexpressing GRK2 (compare Fig. 4, B and D). Importantly, the  $\beta$ 2AR<sup>SSS</sup> mutant receptor still demonstrated a significantly slower rate of dissociation compared with the wild-type  $\beta$ 2AR

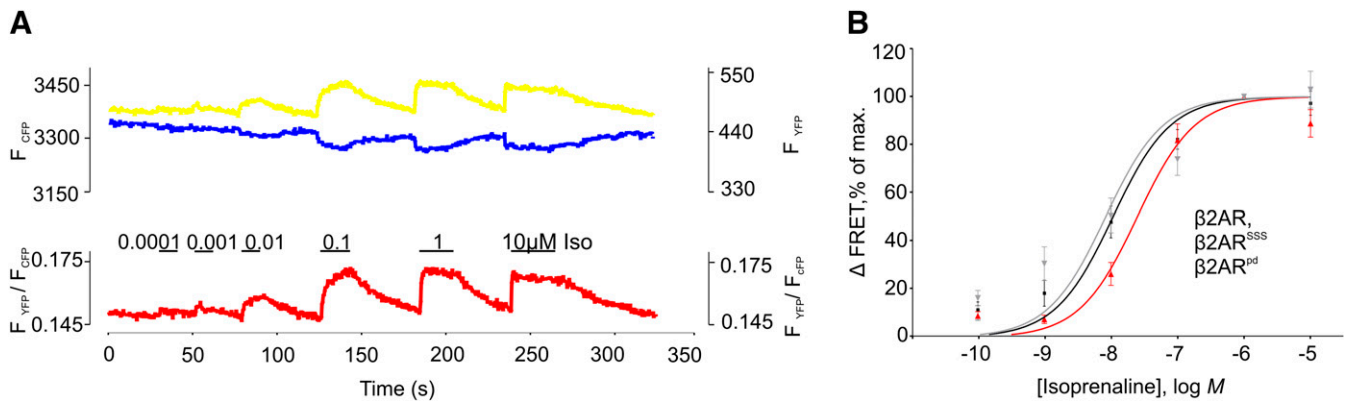


**Fig. 3.** Analysis of receptor G protein interaction by FRET. (A) HEK293T cells transiently expressing  $\beta 2\text{AR}$ -YFP,  $\beta 2\text{AR}^{\text{SSS}}$ -YFP, or  $\beta 2\text{AR}^{\text{pd}}$ -YFP and  $G\alpha_s$ ,  $G\beta_1$ -Cer and  $G\gamma_2$  were stimulated with different concentrations of isoprenaline. Representative FRET traces showing the  $\beta 2\text{AR}$ -YFP interaction with  $G\beta_1$ -Cer upon stimulation with different concentrations of isoprenaline. (B) Concentration-response curves of receptor/G protein interactions for  $\beta 2\text{AR}$ ,  $\beta 2\text{AR}^{\text{SSS}}$ , or  $\beta 2\text{AR}^{\text{pd}}$  ( $n = 7-9$ ) were obtained by evaluating the amplitudes of FRET changes. FRET responses after stimulation with  $1 \mu\text{M}$  isoprenaline were set to 100%. Individual curves to obtain  $\text{EC}_{50}$  values were fitted using a sigmoidal dose response equation with constant hill slope = 1, statistics of obtained  $\text{EC}_{50}$  values was done with an analysis of variance followed by Bonferroni's multiple comparison test  $P = \text{n.s.}$

in the cells expressing endogenous levels of GRK (Fig. 4, C and D; Table 1). We relate the ability of the  $\beta 2\text{AR}^{\text{SSS}}$  to bind arrestin with enhanced affinity to the insertion of the triple S cluster and its phosphorylation. To ascribe the enhanced phosphorylation shown in Fig. 2A to phosphorylation of one or more of the introduced sites we assessed the phosphorylation of a  $\beta 2\text{AR}$  that contains solely the 3S cluster ( $\beta 2\text{AR}$  3S); all other potential GRK phosphorylation sites were mutated to glycine or alanine (see Fig. 1 for sequences). To exclude the possibility of PKA phosphorylation, we stimulated the cells in the presence of the PKA inhibitor KT5720 and compared agonist-dependent receptor phosphorylation between  $\beta 2\text{AR}$  2S,  $\beta 2\text{AR}$  3S,  $\beta 2\text{AR}$  5S, and  $\beta 2\text{AR}$  pd. The  $\beta 2\text{AR}$  3S showed a substantial increase in ligand-dependent phosphorylation that was similar to the increase in the phosphorylation of  $\beta 2\text{AR}$  2S (Fig. 5, A and B), suggesting that at least one or two of the serines within the 3S cluster can become phosphorylated in an agonist-dependent manner. The largest increase in phosphorylation was observed upon stimulation of a receptor that contains Ser 355,356 and the SSS cluster in combination, thereby further confirming the assumption that the triple S cluster serves as a substrate for GRKs. To examine the phosphorylation dependence of arrestin recruitment, we determined the raise in the FRET signal with  $\beta 2\text{AR}$ s with increasing numbers of serines, as described above (Fig. 5C). No direct interaction between arrestin and the  $\beta 2\text{AR}^{\text{pd}}$  could be detected in FRET, confirming previous results (Krasel et al., 2005). However, introducing either  $\text{S}^{355}$  and  $\text{S}^{356}$  or replacing residues 361–363 (GEQ) with SSS both led to a marked increase in FRET that was further enhanced when both serine motifs in combination were present (Fig. 5C). To rule out the possibility that the increase in the amplitude of the FRET signal resulted from unequal relative expression levels of  $\beta 2\text{AR}$ s and arrestin-3, we determined the relative expression levels as described in *Materials and Methods* and as shown in Fig. 5D. We found no significant difference in the stoichiometry of the fluorescently labeled proteins, indicating that the number of phosphorylation sites determines the extent of the arrestin interaction with receptors.

#### Influence of a Distal SSS Cluster on Arrestin Affinity.

To analyze the relevance of the localization of the 3S cluster,

we replaced three residues 397–399 (NID) within the  $\beta 2\text{AR}$  with serines ( $\beta 2\text{AR}$  SSS distal, Fig. 1) and determined the arrestin interaction using FRET. The arrestin dissociation kinetics were very similar for  $\beta 2\text{AR}$  and  $\beta 2\text{AR}$  SSS distal as both traces were superimposable after ligand washout (Supplemental Fig. 1, A and B). The comparison of these data to the dissociation kinetics from the  $\beta 2\text{AR}$  with the SSS cluster in the proximal part of the C-terminal tail (Supplemental Fig. 1B) revealed that arrestin shows enhanced affinity toward a receptor with the proximal SSS cluster but not toward a receptor that offers the same cluster with a total of four consecutive serines in the distal part of the tail.

**Arrestin-Receptor Interaction in the Continuous Presence of Agonist.** During agonist washout, the receptor undergoes a conformational change from an activated into a nonactivated state. Arrestin senses this conformational change and dissociates from the receptor (Krasel et al., 2005). To investigate whether arrestin affinity for the active state of the receptor is changed by the addition of phospho-acceptor sites to the C-terminal tail of the receptor, we established an assay based on dual color fluorescence recovery after photobleaching (FRAP) to monitor the kinetics of association and dissociation of arrestin-3 to agonist-bound  $\beta 2\text{AR}$ ,  $\beta 2\text{AR}^{\text{SSS}}$ , or  $\beta 2\text{V2R}$ . All receptor constructs used in this assay were N-terminally tagged with YFP and were observed in single living cells. Receptors were immobilized at the membrane by cross-linking them with a polyclonal YFP-antibody (Dorsch et al., 2009). Subsequently, receptors were stimulated with  $10 \mu\text{M}$  isoprenaline, causing arrestin-3-CFP translocation to receptors. A small region of interest ( $3 \times 1 \mu\text{m}$ ) at the plasma membrane was photobleached using high laser intensity, and the re-distribution of both immobilized receptors and arrestin-3 was monitored simultaneously using low laser intensity (Fig. 6, A and B). Antibody crosslinking treatment reduced the mobility of the receptors by reducing the lateral diffusion of receptor-arrestin complexes such that receptor recovery was  $\sim 20\%$  for all three receptor constructs (Fig. 6D) compared with more than  $50\%$  for noncrosslinked receptor (Fig. 6F). The recovery of fluorescent arrestin-3 into the bleached area is therefore a result of arrestin-3 dissociation from and reassociation to immobile receptors. We found that this recovery could be quantified by

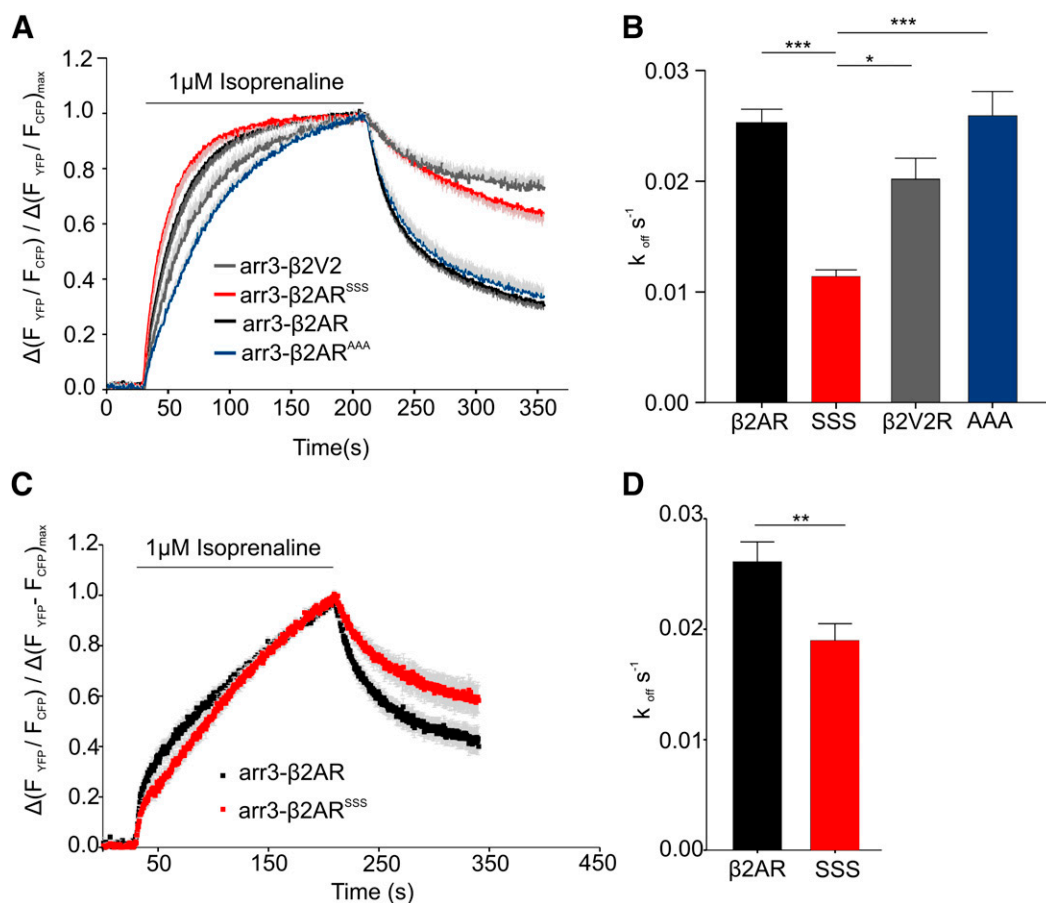


**Fig. 4.** Differential arrestin-3 affinities to  $\beta_2$ -adrenoceptors with varying receptor-C-terminal tails upon agonist washout measured in real time by FRET. (A) Summarized data for arrestin-3 interaction with  $\beta_2$ AR,  $\beta_2$ AR<sup>SSS</sup>,  $\beta_2$ AR<sup>AAA</sup>, or  $\beta_2$ V2R. HEK293T cells were transiently transfected with arrestin-3-CFP, GRK2, and either C-terminally YFP-tagged Flag- $\beta_2$ AR, Flag- $\beta_2$ V2R, Flag- $\beta_2$ AR<sup>SSS</sup>, or Flag- $\beta_2$ AR<sup>AAA</sup>. Dynamics of arrestin-3 interaction with receptors were determined by measuring FRET. Cells were perfused with FRET buffer for 30 seconds, followed by 1  $\mu$ M isoprenaline for 180 seconds, followed by FRET buffer for 180 seconds. On-rates were determined by curve-fitting to a single exponential equation. Statistics were performed by Kruskal Wallis test followed by Dunn's multiple comparison test. \*\*\* $P < 0.001$  ( $\beta_2$ AR<sup>AAA</sup> versus  $\beta_2$ AR<sup>SSS</sup>); \*\* $P < 0.01$  ( $\beta_2$ AR versus  $\beta_2$ AR<sup>AAA</sup>). (B) Calculated  $k_{\text{off}} \pm$  S.E. of arrestin-3 (arr-3)-receptor dissociation upon agonist washout. Off-rates were fitted to a single exponential equation and statistics were performed by Kruskal Wallis test followed by Dunn's multiple comparison test. \*\*\* $P < 0.001$ , \*\* $P < 0.01$ , \* $P < 0.05$ . (C) HEK 293T cells transiently transfected with  $\beta_2$ AR-YFP or  $\beta_2$ AR<sup>SSS</sup>-YFP and arr-3-CFP were measured and the data are summarized as described in (A). (D)  $k_{\text{off}} \pm$  S.E., Student's  $t$  test, \*\* $P < 0.01$ .

a two-phase association. Figure 6C shows the mean recovery  $\pm$  S.E. of arrestin-3 with  $\beta_2$ AR,  $\beta_2$ AR<sup>SSS</sup>, or  $\beta_2$ V2R, and Table 2 summarizes the time constants  $k_{\text{fast}}$ ,  $k_{\text{slow}}$ , and corresponding  $t_{0.5}$  values as well as the extent of the arrestin-3 recovery. The three  $\beta_2$ AR constructs all showed differences in the kinetics of arrestin-3 recovery. The slow recovery rate of arrestin-3 for the  $\beta_2$ AR<sup>SSS</sup> construct was reduced about 1.5-fold compared with the  $\beta_2$ AR (Fig. 6D), whereas the extent of recovery was

unchanged. In contrast, the recovery rate for the  $\beta_2$ V2R was slowed down more than 3-fold compared with the  $\beta_2$ AR, and the extent of recovery was reduced 2.5-fold compared with the  $\beta_2$ AR (Fig. 6, B and D; Table 2).

In addition, we determined the arrestin-3 recovery after photobleaching to Flag- $\beta_2$ AR or Flag- $\beta_2$ AR<sup>SSS</sup> on  $\mu$ -patterned surfaces using total internal reflection fluorescence (TIRF) microscopy in HeLa cells to study the mobility of arrestin-3

TABLE 1

Kinetic constants of FRET experiments for arrestin-3 (arr-3) interaction with various receptors

$k_{\text{on}}$ ,  $k_{\text{off}}$ , and  $t_{0.5}$  of arrestin association and dissociation as well as the portion of arrestin dissociation were obtained by monoexponential curve fitting as described in *Materials and Methods*. Association rates of arrestin without GRK2 overexpression could not be determined by curve fitting as the plateau was not reached during the timescale of the experiment.

FRET	$k_{\text{on}} \pm$ S.E.	$k_{\text{off}} \pm$ S.E.	$t_{0.5 \text{ on}}$	$t_{0.5 \text{ off}}$	Portion of arr-3 Dissociation $\pm$ S.E.
	second <sup>-1</sup>		seconds		%
$\beta_2$ AR (+GRK2)	0.040 $\pm$ 0.004	0.025 $\pm$ 0.001	17.3	27.7	69.1 $\pm$ 2.1
$\beta_2$ AR AAA (+GRK2)	0.017 $\pm$ 0.002	0.026 $\pm$ 0.002	40.8	26.7	65.3 $\pm$ 3.2
$\beta_2$ AR SSS (+GRK2)	0.061 $\pm$ 0.008	0.011 $\pm$ 0.0007	11.4	63.0	36.1 $\pm$ 3.1
$\beta_2$ V2R (+GRK2)	0.026 $\pm$ 0.004	0.020 $\pm$ 0.002	26.7	34.7	27.4 $\pm$ 4.9
$\beta_2$ AR	n.a.	0.026 $\pm$ 0.002	n.a.	26.7	59.1 $\pm$ 5.1
$\beta_2$ AR <sup>SSS</sup>	n.a.	0.019 $\pm$ 0.002	n.a.	36.5	41.7 $\pm$ 5.6

n.a., Not applicable.

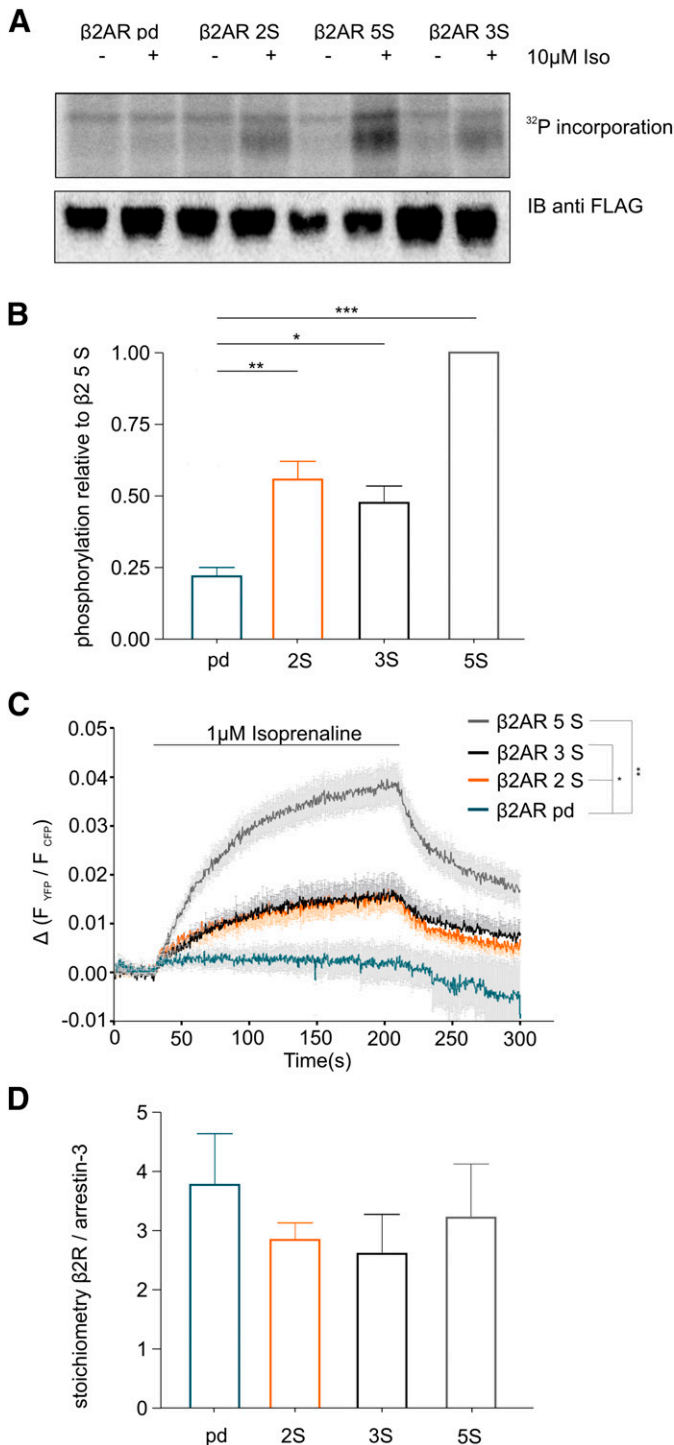


**Fig. 5.** Number of phosphorylation sites within the  $\beta$ 2AR determines the extent of ligand dependent interaction of arrestin-3. (A) HEK 293T cells transiently expressing  $\beta$ 2 receptors with the indicated number of possible phosphorylation sites were preincubated for 30 minutes with 1  $\mu$ M of the PKA inhibitor KT 5720 ((9R,10S,12S)-2,3,9,10,11,12-hexahydro-10-hydroxy-9-methyl-1-oxo-9,12-epoxy-1H-diindolo[1,2,3-fg:3',2',1'-kl]pyrrolo[3,4-i][1,6]benzo-diazocine-10-carboxylic acid hexyl ester). Isoprenaline-challenged receptors were immunoprecipitated and phosphorylated proteins were visualized by autoradiography (upper panel); receptor expression was shown by Western blotting (lower panel). (B) Quantification of ligand-induced phosphorylation as presented in (A). Results are mean  $\pm$  S.E. of three independent experiments, \*\*\* $P$  < 0.001; \*\* $P$  < 0.01; \* $P$  < 0.05. Analysis of variance (ANOVA) followed by Bonferroni's multiple comparison test. (C) HEK 293T cells were transiently transfected with the indicated YFP-labeled receptors, arrestin-3 CFP and GRK2. Individual single-cell recordings of agonist-induced alterations in

clusters at the cell surface. Figure 7A shows an example of  $\mu$ -patterned Flag- $\beta$ 2AR-CFP. Unstimulated receptors (Fig. 7A, upper panel) showed low levels of arrestin-3 clustering of arrestin-3, whereas arrestin-3 clustering was robustly increased upon stimulation with 10  $\mu$ M isoprenaline (Fig. 7A, lower panel). Increased clustering and colocalization of arrestin-3 in receptor-enriched  $\mu$ -patterns was quantified by contrast evaluation (Fig. 7B). The arrestin-3-YFP recovery after photo-bleaching was slowed 3-fold for the  $\beta$ 2AR<sup>SSS</sup> compared with  $\beta$ 2AR (Fig. 7C, upper panel versus lower panel, and D and E).

**Arrestin-3 Trafficking.** We next set out to investigate how the introduction of additional phospho-acceptor sites within the  $\beta$ 2AR C terminus might change the trafficking pattern of arrestin-3. Isoprenaline stimulation of YFP-tagged  $\beta$ 2AR,  $\beta$ 2AR<sup>SSS</sup>, or  $\beta$ 2V2R increased receptor internalization in all cases (Fig. 8A, middle panel). After 30 minutes of  $\beta$ 2AR stimulation, arrestin-3 was found either redistributed into the cytosol or at or near to the plasma membrane (Fig. 8A, upper panel, left), whereas upon  $\beta$ 2AR<sup>SSS</sup> or  $\beta$ 2V2R activation arrestin was found on intracellular vesicles (Fig. 8A, middle and lower left panel). The intracellular cotrafficking of arrestin with receptors was quantified by using Pearson's correlation coefficient as described in *Materials and Methods*. Quantification of the cotrafficking showed that the endocytic colocalization of arrestin with  $\beta$ 2AR<sup>SSS</sup> and the  $\beta$ 2V2R as a control was markedly enhanced compared with  $\beta$ 2AR (Fig. 8B).

To further characterize the arrestin-3 trafficking,  $\beta$ 2AR,  $\beta$ 2AR<sup>SSS</sup>, or  $\beta$ 2V2R was stimulated with isoprenaline and arrestin-3 was analyzed for colocalization with early endosome antigen 1 (EEA1), which is a specific marker for early endosomes (Stenmark et al., 1996). Stimulation of the  $\beta$ 2AR with 10  $\mu$ M isoprenaline resulted in translocation of arrestin-3-CFP to the plasma membrane that remained unchanged over a 30-minute period of observation (Fig. 9A, upper panel). In contrast, stimulation of the  $\beta$ 2AR<sup>SSS</sup> (Fig. 9A, middle panel) and  $\beta$ 2V2R (Fig. 9A, lower panel) caused internalization of arrestin-3-CFP into EEA1-positive compartments. Colocalization was quantified using Pearson's correlation coefficient and identified significant differences between arrestin-3 trafficking with  $\beta$ 2AR<sup>SSS</sup> and  $\beta$ 2V2R compared with  $\beta$ 2AR (Fig. 9B).

To clarify whether the presence of the triple S cluster in combination with Ser 355/356 ( $\beta$ 2AR 5S) is able to induce endosomal cotrafficking with arrestin, we performed additional trafficking experiments with this mutant (Supplemental Fig. 2). After 30 minutes of agonist incubation, little overlap of arrestin with EEA1 could be observed (Supplemental Fig. 2, lower panel). These data suggest that the SSS cluster is required in addition to the full pattern of serines and threonines in the proximal part of the tail but not sufficient for the cointernalization of arrestin and  $\beta$ 2AR.

**Internalization and Recycling of  $\beta$ 2AR and  $\beta$ 2AR<sup>SSS</sup>.** We next investigated whether the enhanced arrestin affinity toward the SSS cluster in the proximal part of the  $\beta$ 2AR was

FRET between arrestin-3 and different  $\beta$ 2AR mutants were averaged (mean  $\pm$  S.E.;  $n \geq 6$ ) and are shown as absolute alterations in FRET. For better visualization mean curves for  $\beta$ 2AR 3S or  $\beta$ 2AR 2S are displayed with S.E. of  $\Delta(F_{YFP}/F_{CFP})$  in one direction. \*\*\* $P$  < 0.01; \* $P$  < 0.5; ANOVA followed by Dunnett's multiple comparison test. (D) Relative expression levels of  $\beta$ 2AR mutants and arrestin-3, as measured by comparing CFP and YFP fluorescence, were not significantly different between the conditions.

TABLE 2

Kinetic constants of FRAP experiments for arrestin-3 (arr-3) interaction with various receptors

The kinetic parameters  $k_{\text{on fast}}$  and  $k_{\text{on slow}}$  of FRAP experiments were obtained by biexponential curve fitting.  $t_{0.5}$  values were obtained by calculating  $\ln(2)/k$ .

	arr-3 recovery $\pm$ S.E.	$k_{\text{fast}} \pm$ S.E.	$k_{\text{slow}} \pm$ S.E.	Fast half-life	Slow half-life
	%	$\text{second}^{-1}$		seconds	
FRAP Confocal					
$\beta$ 2AR	54.6 $\pm$ 2.6	0.185 $\pm$ 0.015	0.019 $\pm$ 0.001	3.8	36.5
$\beta$ 2AR <sup>SSS</sup>	51.3 $\pm$ 5.1	0.085 $\pm$ 0.017	0.012 $\pm$ 0.001	8.2	57.8
$\beta$ 2V2R	21.3 $\pm$ 2.7	0.143 $\pm$ 0.038	0.006 $\pm$ 0.001	4.9	115.5
FRAP TIRF					
$\beta$ 2AR	70.3 $\pm$ 1.5	0.187 $\pm$ 0.023	0.016 $\pm$ 0.003	3.70	42.13
$\beta$ 2AR <sup>SSS</sup>	75.2 $\pm$ 3.9	0.270 $\pm$ 0.170	0.004 $\pm$ 0.0003	2.56	152

associated with altered internalization or recycling of receptors. Ligand-dependent internalization of the  $\beta$ 2AR is an arrestin-dependent process; therefore we hypothesized that a receptor that possesses the ability to bind arrestin stronger might show alterations in its internalization properties. Indeed, the  $\beta$ 2AR<sup>SSS</sup> internalized significantly more efficiently (30  $\pm$  4.5%) than the wild-type receptor (13.5  $\pm$  4.6%; Fig. 10A) after 30 minutes of treatment with 1  $\mu$ M isoprenaline. Similar results for  $\beta$ 2AR internalization in the absence of overexpressed arrestin have been published before (Kim and Benovic, 2002). After 30 minutes of stimulation, the agonist was removed by repetitive washing steps, and receptors were allowed to recycle for the indicated time points (Fig. 10). Both  $\beta$ 2AR and  $\beta$ 2AR<sup>SSS</sup> recycled rapidly by  $\sim$ 60% within 30 minutes. Very similar results for the recycling of wild-type  $\beta$ 2AR without subsequent antagonist treatment were observed before (Gage et al., 2001).

## Discussion

For many GPCRs, agonist-dependent receptor phosphorylation results in arrestin recruitment and subsequent internalization. Arrestin can either dissociate from the receptor very shortly after internalization, giving the appearance of plasma membrane staining, or cointernalize with the receptor into endosomes. Based on work with receptor chimeras, it has been suggested that this trafficking behavior depends on the number of Ser and/or Thr residues in the C terminus of the receptor (Oakley et al., 2000; Pal et al., 2013). However, swapping the entire C terminus of the receptor will not only affect arrestin trafficking but other receptor properties as well, such as recycling (Cao et al., 1999). Therefore we examined whether the insertion of just three additional serine phospho-acceptor sites 20 amino acids away from the plasma membrane ( $\beta$ 2AR<sup>SSS</sup>) could induce any changes regarding receptor phosphorylation, arrestin affinity, and trafficking. First, we investigated whether the addition of three serines within the  $\beta$ 2AR<sup>SSS</sup> leads to an increase in total receptor phosphorylation. Second, we monitored G protein coupling, arrestin-3 recruitment, and dissociation in real time. In addition, we analyzed arrestin-3 trafficking behavior as well as receptor internalization and recycling in response to this mutation. We demonstrate that the addition of phospho-acceptor sites to the proximal C terminus of the  $\beta$ 2AR led to increased agonist-induced phosphorylation that was accompanied by enhanced stability of arrestin-3-receptor complexes and arrestin-3 localization on endosomes.

Using FRET, we measured the interaction of heterotrimeric G proteins with  $\beta$ 2AR in a dose-dependent manner and found no significant differences for the EC<sub>50</sub> values of isoprenaline-induced G protein interaction with  $\beta$ 2AR,  $\beta$ 2AR<sup>SSS</sup>, or  $\beta$ 2AR<sup>pd</sup> (Fig. 3). These results suggest that the initial phase of G protein coupling occurs independently from receptor phosphorylation and compare favorably with those reported in the literature (Benovic et al., 1987; Lohse et al., 1992).

The real-time observation of arrestin-3 recruitment using FRET revealed that upon stimulation with 1  $\mu$ M isoprenaline, arrestin-3 was recruited to  $\beta$ 2AR,  $\beta$ 2AR<sup>SSS</sup>,  $\beta$ 2AR<sup>AAA</sup>, or  $\beta$ 2V2R. The differing recruitment kinetics probably reflect subtle differences in the ability of the various receptors to be phosphorylated by GRK2. During agonist washout, the receptor undergoes a conformational change from an activated into a nonactivated state. Arrestin is able to sense this conformational change and dissociates from the receptor (Krasel et al., 2005). The arrestin-3 dissociation kinetics from a typical class A receptor, such as the  $\beta$ 2AR, proceeded quickly and almost completely, whereas the dissociation rate from the class B receptor  $\beta$ 2V2R (Oakley et al., 1999) was delayed and considerably smaller (Fig. 4A). Interestingly, the interaction of arrestin-3 with the  $\beta$ 2AR<sup>SSS</sup> construct was significantly prolonged by a factor of 2.5, and the fraction of arrestin that dissociated after ligand washout was reduced by half. Hence, the kinetic data presented here provide some evidence that different phosphorylation states of receptors can be detected by arrestin-3 and these are reflected in the arrestin dissociation rate that we measured here in real time. Because the affinity to the receptor remained unchanged by the addition of a SSS cluster to the distal part of the tail (Supplemental Fig. 1), this confirms that arrestin senses phosphorylation specifically in the proximal part of the C-terminal tail.

We extended our study further by asking whether the addition of phospho-acceptor sites to the receptor C-tail can also alter the arrestin-3 affinity for the activated receptor. Dual color fluorescence recovery after photobleaching (FRAP) was used here to monitor the kinetics of association and dissociation of arrestin-3 to immobilized agonist-bound  $\beta$ 2AR,  $\beta$ 2V2R, and  $\beta$ 2AR<sup>SSS</sup> in single living cells. The arrestin-3 recovery after photobleaching reflects two processes, the remaining lateral diffusion of receptor–arrestin-3 complexes and the release of arrestin-3 from immobilized receptors followed by subsequent rebinding of free arrestin-3. The  $\beta$ 2AR<sup>SSS</sup> showed approximately 2.2-fold slower fluorescence recovery than the  $\beta$ 2AR in HEK293 cells using confocal microscopy and approximately 4-fold slower fluorescence recovery in HeLa cells using TIRF



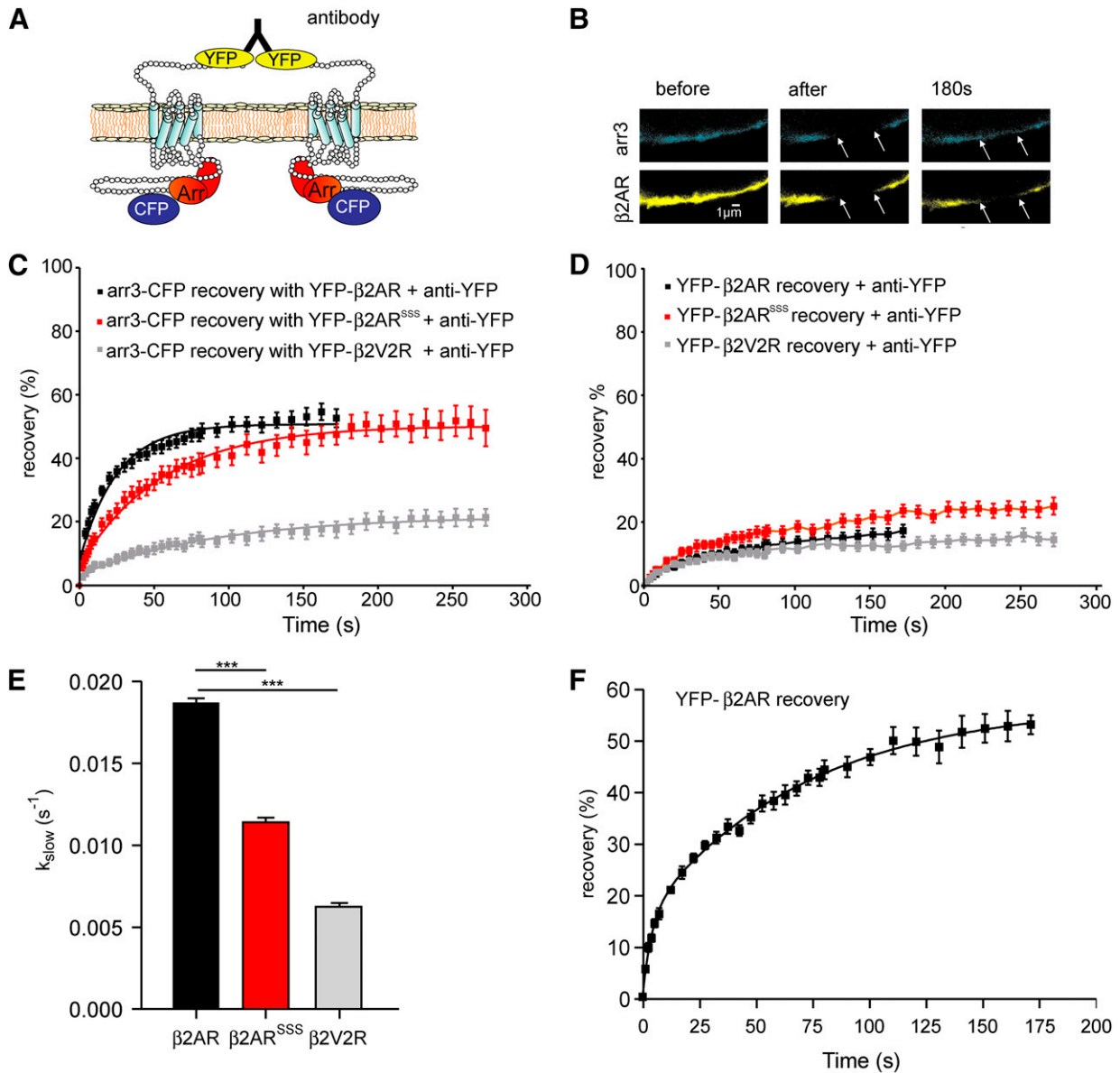


**Fig. 6.** Arrestin-3 mobility determined by dual color FRAP in the continuous presence of agonist. HEK 293T cells were transiently transfected with either  $\beta 2\text{AR}$ ,  $\beta 2\text{V}2\text{R}$  chimera, or  $\beta 2\text{AR}^{\text{SSS}}$  tagged N terminally with YFP and arrestin-3-CFP. Cells were preincubated with a polyclonal anti-YFP antibody for 30 minutes at 37°C before being stimulated with 10  $\mu\text{M}$  isoprenaline. (A and B) Arrestin-3-CFP and YFP-tagged receptors were photobleached in a small spot (white arrows) at the membrane by high confocal laser intensities, and redistribution of both was measured for at least 180 seconds using low laser intensities. The scale bar represents 1  $\mu\text{m}$ . Mean recovery for arrestin-3 (C) or receptors (D) was calculated ( $n = 17\text{--}23$ ),  $k_{\text{fast}}$  and  $k_{\text{slow}}$  were fitted to a biphasic exponential equation as described in *Materials and Methods*. Mean recovery and corresponding  $t_{0.5}$  values are summarized in Table 2. (E)  $k_{\text{slow}} \pm \text{S.E.}$  \*\*\* $P < 0.001$ , analysis of variance followed by Dunnett's multiple comparison test. (F) Recovery of YFP- $\beta 2\text{AR}$  without anti-YFP pretreatment.

microscopy. These differences in the kinetics and the extent of arrestin-3-recovery in the equatorial plane of the membrane or at the cell surface reflect its stability in complex with the various receptors investigated in this study. Thus, the temporal stability of arrestin-3-receptor complexes in the presence or in the absence of agonist is determined by the extent and possibly the pattern of receptor phosphorylation that is present in the proximal part of the receptor's C-terminal tail. The slow kinetics of arrestin-3 recovery for the  $\beta 2\text{AR}^{\text{SSS}}$  were more pronounced using TIRF microscopy. We assume that this could be related to the larger area that was photobleached on the cell surface (7  $\mu\text{m}^2$ , circle) compared with area that was photobleached within the equatorial plane of the membrane (3  $\times$  1  $\mu\text{m}$ , rectangle).

We and others have shown that the number of phosphorylated residues on receptors determines the nature of the complex formed with arrestins (Vishnivetskiy et al., 2007; Krasel et al., 2008). The kinetic modeling of arrestin-3 with  $\beta 2\text{AR}$  or  $\beta 2\text{AR}^{\text{SSS}}$  via FRET or FRAP suggests that very likely the phosphorylation of the additional serine cluster leads to a 2- to 4-fold enhancement in the stability of the complex between arrestin-3 and  $\beta 2\text{AR}^{\text{SSS}}$  compared with the nature of the complex formed with  $\beta 2\text{AR}$  that appears to be rather transient. Different phosphorylation patterns elicited by different GRKs or arising from stimulation with distinct ligands have been proposed to impart differential arrestin conformations responsible for the fine-tuning of subsequent signaling events (Nobles et al., 2011). We show here that the

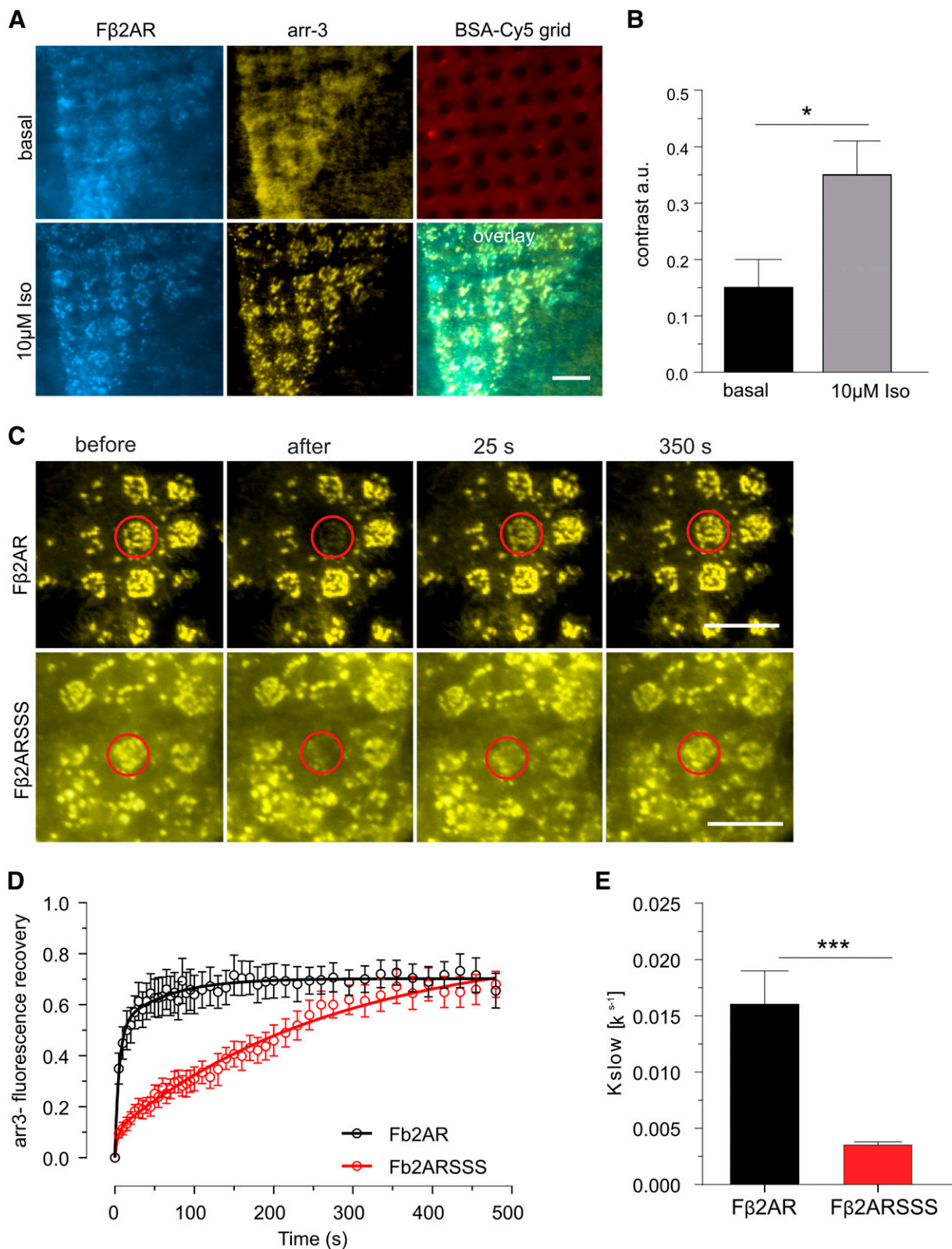


**Fig. 7.**  $\mu$ -Patterning for quantification of arr-3 mobility with  $\beta$ 2AR and  $\beta$ 2AR<sup>SSS</sup> via TIRF microscopy. HeLa cells transiently expressing Flag- $\beta$ 2AR-CFP, GRK2 and YFP-arr-3 were grown on a  $\mu$ -biochip coated with anti-Flag antibodies. (A) Accurate alignment of anti-Flag antibodies into unblocked spots leads to enrichment of the bait protein ( $\beta$ 2AR) into  $\mu$ -patterns. Colocalization of the prey protein (arr-3) in anti-Flag antibody-positive regions indicated specific protein-protein interactions. Stimulation with 10  $\mu$ M isoprenaline significantly increased the basic fluorescent contrast for arr-3. (B) Quantification of  $\beta$ 2AR-arr-3 interaction by contrast evaluation. \* $P < 0.05$ , Student's  $t$  test. (C) Photobleaching experiments on  $\mu$ -biochips. Individual arrestin-3 patterns were selected for the FRAP experiment. Images show a representative cell with a single bleached spot before and at the indicated time points after photobleaching for  $\beta$ 2AR (upper panel) and  $\beta$ 2AR<sup>SSS</sup> (lower panel). Scale bars represent 10  $\mu$ m. (D) Normalized mean recovery curves for arrestin-3 were calculated ( $n = 17$  for each condition),  $k_{fast}$  and  $k_{slow}$  were fitted to a biphasic exponential equation as described in *Materials and Methods*. (E)  $k_{slow} \pm$  S.E. \*\*\* $P < 0.001$  with Student's  $t$  test.

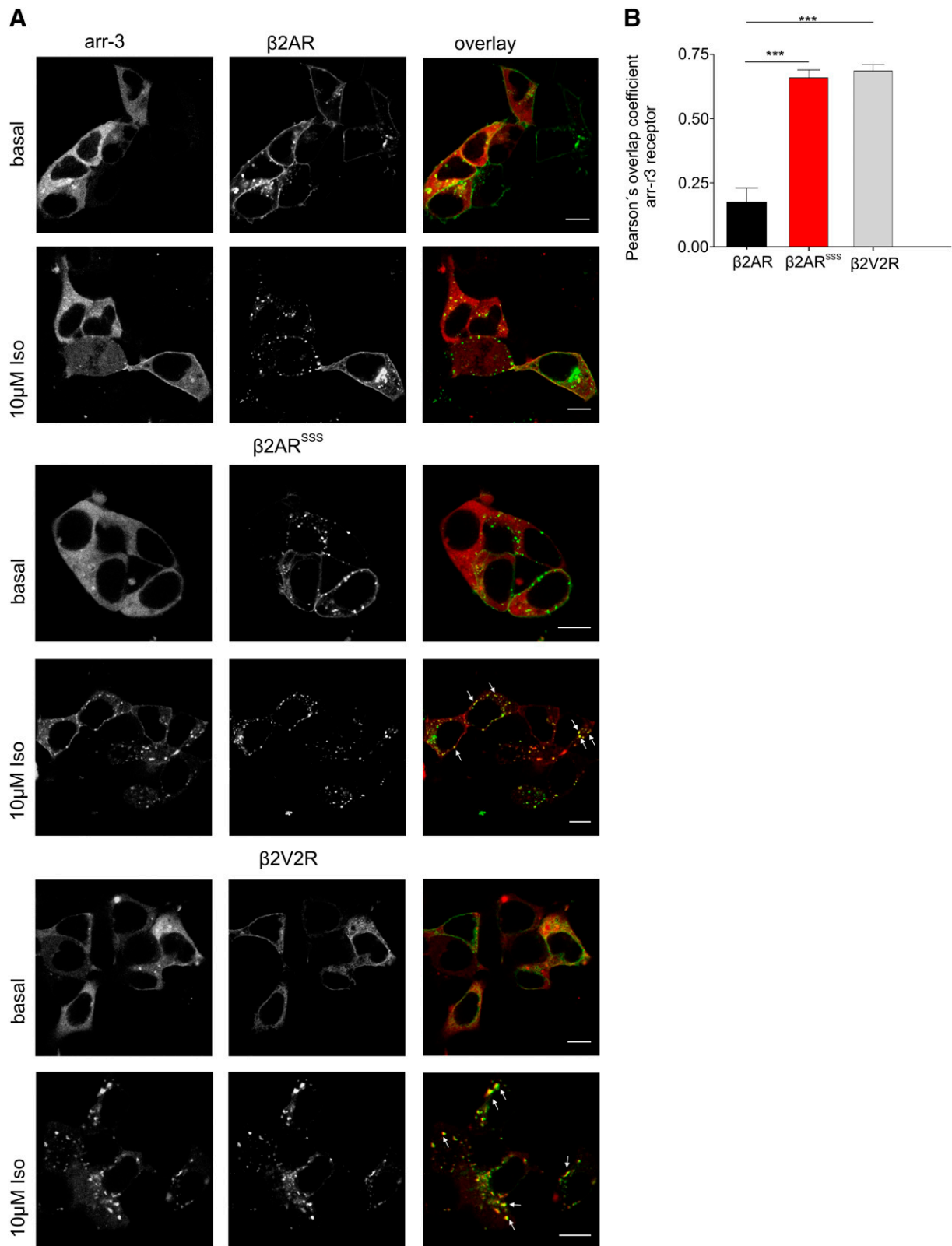


**Fig. 8.** Cellular trafficking of arrestin-3 with  $\beta 2AR$ ,  $\beta 2AR^{SSS}$ , and  $\beta 2V2R$ . (A) HEK 293T cells were transiently transfected with YFP-labeled  $\beta 2AR$ ,  $\beta 2AR^{SSS}$  or  $\beta 2V2R$ , arrestin-3-CFP, and GRK2. Cells were stimulated or not for 30 minutes with 10  $\mu M$  isoprenaline at 37°C, fixed, and imaged by confocal microscopy. The scale bars represent 10  $\mu m$ .  $\beta 2AR$ ,  $\beta 2AR^{SSS}$ , or  $\beta 2V2R$  appeared mostly at the plasma membrane under basal conditions, whereas arrestin-3 appeared mostly in the cytoplasm. After isoprenaline treatment internalized receptors were observed as punctate staining on the membrane or in the cytoplasm. Colocalized receptor and arrestin-3 are observed as yellow spots (arrows) when the images are merged. (B) Pearson's correlation coefficient calculated for colocalization of arrestin-3-CFP and indicated YFP-labeled receptors (mean  $\pm$  S.E.;  $n \geq 7$ ). \*\*\* $P < 0.001$ , analysis of variance followed by Bonferroni's multiple comparison test.

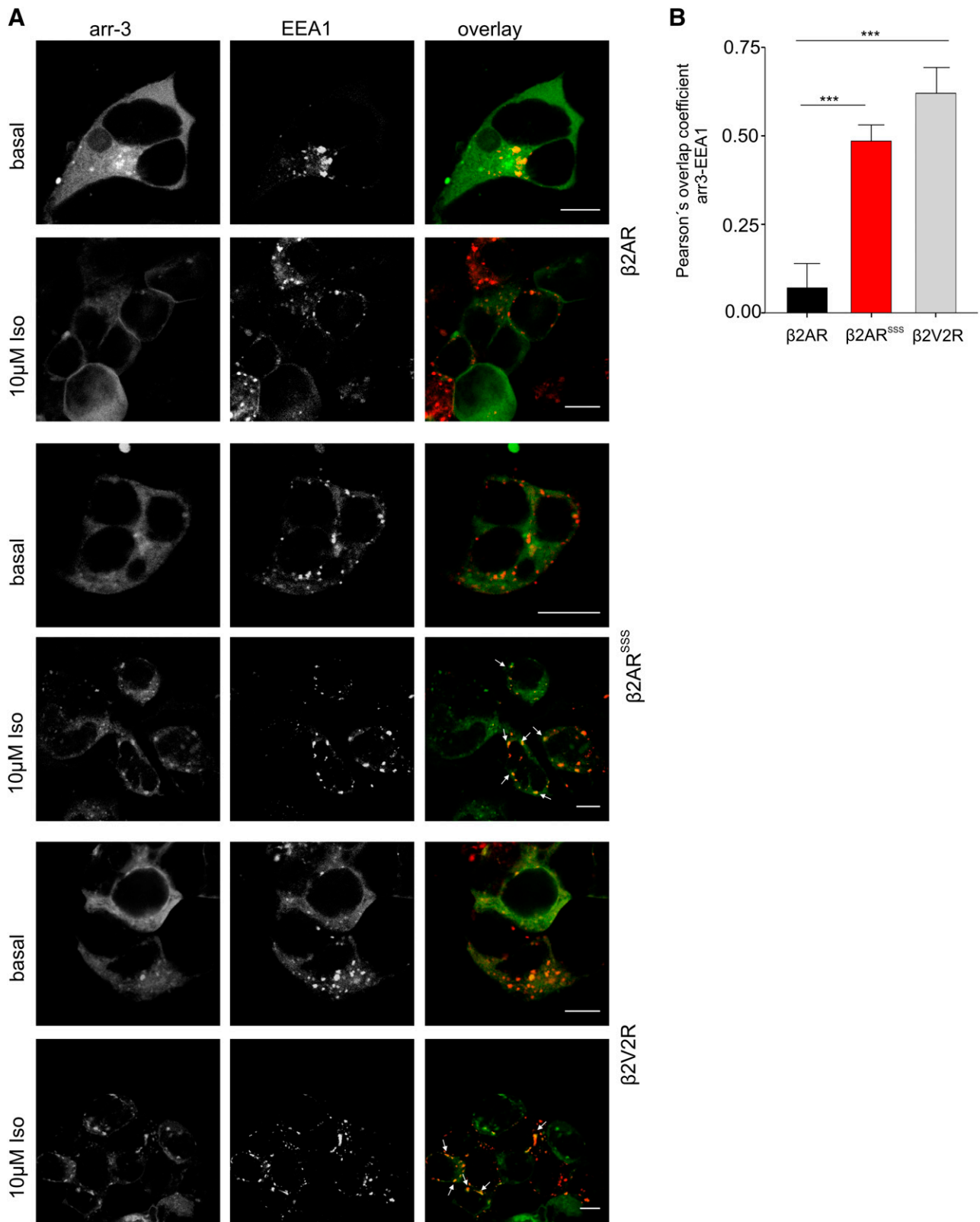


**Fig. 9.** Colocalization of arrestin-3 with EEA1 after  $\beta$ 2AR,  $\beta$ 2AR<sup>SSS</sup>, and  $\beta$ 2V2R stimulation. (A) Confocal images of HEK 293T cells transiently expressing  $\beta$ 2AR,  $\beta$ 2AR<sup>SSS</sup> or  $\beta$ 2V2R, arr-3-CFP, GRK2, and mCherry-EEA1. Cells were stimulated or not with 10  $\mu$ M isoprenaline for 30 minutes at 37°C, fixed, and analyzed for colocalization of arrestin-3 and EEA1. Scale bar represents 10  $\mu$ m. (B) Pearson's correlation coefficients calculated for arrestin-3-CFP and mCherry-EEA1 colocalization ( $n = 7-10$ ), mean  $\pm$  S.E. \*\*\* $P < 0.001$ , analysis of variance followed by Bonferroni's multiple comparison test.

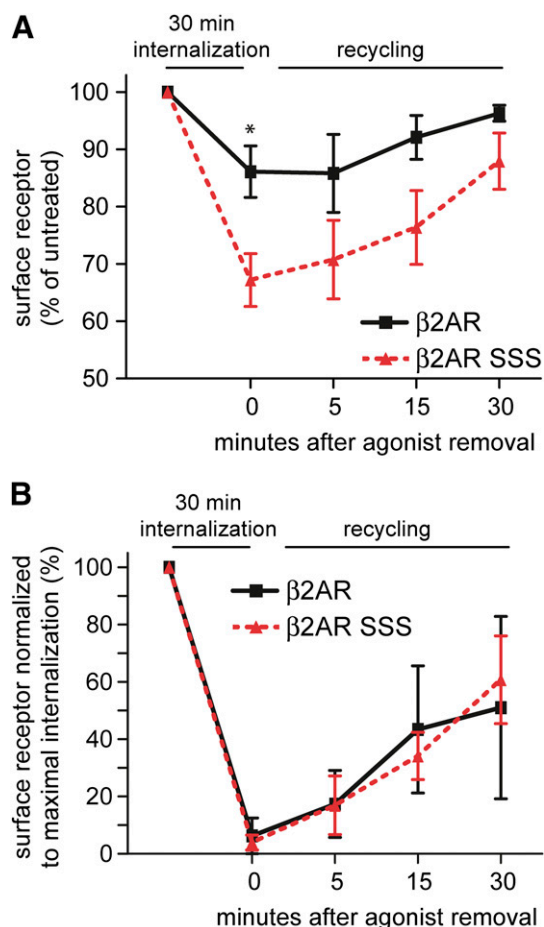


**Fig. 10.** Agonist-induced receptor internalization and recycling after agonist removal. (A) HEK 293T cells transiently transfected with  $\beta 2AR$  or  $\beta 2AR^{SSS}$  were stimulated with 1  $\mu M$  isoprenaline for 30 minutes at 37°C. Internalization after 30 minutes was significantly different between  $\beta 2AR$  and  $\beta 2AR^{SSS}$ . \* $P < 0.05$ , Student's  $t$  test. After agonist removal on ice receptors were allowed to recycle for the indicated time points at 37°C. Receptor surface expression was measured as described under *Materials and Methods*. Points represent mean surface receptor recovery  $\pm$  S.E., normalized to the maximum of receptor expression before receptor stimulation. (B) To compare the kinetics of recycling, the recovery of  $\beta 2AR$  or  $\beta 2AR^{SSS}$  to the plasma membrane was normalized to the receptor surface expression before ligand treatment as a maximum and to the maximal internalization after ligand stimulation as a minimum.

removal of all phospho-sites in the proximal C terminus almost abolishes arrestin binding, whereas arrestin interaction was restored to some extent by the addition of two or three phospho-sites; it did not seem to play a role in which exact position these serines were present, as the extent of arrestin interaction was very similar for  $\beta 2AR$  2S and  $\beta 2AR$  3S. The combination of the 3S cluster and Ser 355/356 ( $\beta 2AR$  5S) improved arrestin binding markedly; however, the arrestin affinity was less pronounced with  $\beta 2AR$  5S compared with  $\beta 2AR^{SSS}$ , suggesting that the full range of serines in addition to the SSS cluster is required to switch the characteristics of this receptor. The  $\beta 2AR^{SSS}$  mutant appeared to show characteristics of a class B receptor, a class of GPCRs that were previously proposed to interact strongly with arrestin (Oakley et al., 2000). Previous studies showed that the  $\beta 2AR$  could be converted from a class A to a class B receptor by substituting the C-terminal tail of the receptor with the C-tail of the V2-vasopressin receptor (Oakley et al., 1999). Arrestin-3

dissociates from this chimeric receptor more quickly than from the  $\beta 2AR^{SSS}$  mutant, and both mutants show a reduced extent of arrestin dissociation on the timescale of the experiment compared with wild type (Fig. 4, A and B), supporting the notion that by increasing the number of phosphorylation sites on the  $\beta 2AR$  the receptor is converted from a class A to a class B receptor. Although the  $\beta 2AR^{SSS}$  showed class B behavior in terms of arrestin binding it did not in terms of recycling. However, it was shown previously (Cao et al., 1999) that rapid recycling of the  $\beta 2AR$  was mediated by binding of EPB50 to phosphorylated Ser 411 and the PDZ domain in the distal part of the C-terminal tail; because the distal part was not changed in the  $\beta 2AR^{SSS}$  it is not unexpected that this receptor displays the same recycling properties as the wild-type receptor.

Our data suggest that arrestin can form structurally and functionally differential complexes dependent on the number of phosphorylation sites in the proximal part of the C-terminal tail. In summary, the experiments in this report demonstrate that a 2- to 4-fold increase in the stability of the arrestin-3- $\beta 2AR^{SSS}$  interaction compared with the stability of  $\beta 2AR$ -arrestin-3 complex has a profound impact on the internalization behavior of  $\beta 2AR^{SSS}$  and its trafficking properties with arrestin-3.

#### Acknowledgments

The authors thank Nicholas Holliday and Simon Davies (University of Nottingham) for providing the cDNA for EEA1-GFP. The authors also thank Gerhard Schrott and Christian Wrocklage for access to the isotope laboratory and to the Leica SP5 microscope.

#### Authorship Contributions

Participated in research design: Zindel, Butcher, Al-Sabah, Weghuber, Tobin, Bünemann, Krasel.

Conducted experiments: Zindel, Butcher, Lanzerstorfer, Krasel.

Contributed new reagents or analytic tools: Zindel, Al-Sabah, Krasel.

Performed data analysis: Zindel, Lanzerstorfer, Bünemann, Krasel.

Wrote or contributed to the writing of the manuscript: Zindel, Butcher, Tobin, Krasel.

#### References

- Benovic JL, Kühn H, Weyand I, Codina J, Caron MG, and Lefkowitz RJ (1987) Functional desensitization of the isolated beta-adrenergic receptor by the beta-adrenergic receptor kinase: potential role of an analog of the retinal protein arrestin (48-kDa protein). *Proc Natl Acad Sci USA* **84**:8879–8882.
- Bodmann EL, Rinne A, Brandt D, Lutz S, Wieland T, Grosse R, and Bünemann M (2014) Dynamics of G $\alpha_q$ -protein-p63RhoGEF interaction and its regulation by RGS2. *Biochem J* **458**:131–140.
- Borgmann DM, Weghuber J, Schaller S, Jacak J, and Winkler SM (2012) Identification of patterns in microscopy images of biological samples using evolution strategies, in *Proceedings of the 24<sup>th</sup> European Modeling and Simulation Symposium*; Vienna. pp 271–276.
- Bouvier M, Hausdorff WP, De Blasi A, O'Dowd BF, Kobilka BK, Caron MG, and Lefkowitz RJ (1988) Removal of phosphorylation sites from the  $\beta_2$ -adrenergic receptor delays onset of agonist-promoted desensitization. *Nature* **333**:370–373.
- Butcher AJ, Prihandoko R, Kong KC, McWilliams P, Edwards JM, Bottrill A, Mistry S, and Tobin AB (2011) Differential G-protein-coupled receptor phosphorylation provides evidence for a signaling bar code. *J Biol Chem* **286**:11506–11518.
- Cao TT, Deacon HW, Reczek D, Bretscher A, and von Zastrow M (1999) A kinase-regulated PDZ-domain interaction controls endocytic sorting of the  $\beta_2$ -adrenergic receptor. *Nature* **401**:286–290.
- Digby GJ, Lober RM, Sethi PR, and Lambert NA (2006) Some G protein heterotrimer physically dissociate in living cells. *Proc Natl Acad Sci USA* **103**:17789–17794.
- Doan T, Mendez A, Detwiler PB, Chen J, and Rieke F (2006) Multiple phosphorylation sites confer reproducibility of the rod's single-photon responses. *Science* **313**:530–533.
- Dorsch S, Klotz K-N, Engelhardt S, Lohse MJ, and Bünemann M (2009) Analysis of receptor oligomerization by FRAP microscopy. *Nat Methods* **6**:225–230.
- Frank M, Thümer L, Lohse MJ, and Bünemann M (2005) G Protein activation without subunit dissociation depends on a G $\alpha_i$ -specific region. *J Biol Chem* **280**:24584–24590.
- Gage RM, Kim K-A, Cao TT, and von Zastrow M (2001) A transplantable sorting signal that is sufficient to mediate rapid recycling of G protein-coupled receptors. *J Biol Chem* **276**:44712–44720.
- Hall RA, Premont RT, Chow CW, Blitzer JT, Pitcher JA, Claing A, Stoffel RH, Barak LS, Shenolikar S, and Weinman EJ et al. (1998) The  $\beta_2$ -adrenergic receptor

- interacts with the Na<sup>+</sup>/H<sup>+</sup>-exchanger regulatory factor to control Na<sup>+</sup>/H<sup>+</sup> exchange. *Nature* **392**:626–630.
- Hein P, Rochais F, Hoffmann C, Dorsch S, Nikolaev VO, Engelhardt S, Berlot CH, Lohse MJ, and Bünemann M (2006) G<sub>s</sub> activation is time-limiting in initiating receptor-mediated signaling. *J Biol Chem* **281**:33345–33351.
- Karoor V, Wang L, Wang HY, and Malbon CC (1998) Insulin stimulates sequestration of β-adrenergic receptors and enhanced association of β-adrenergic receptors with Grb2 via tyrosine 350. *J Biol Chem* **273**:33035–33041.
- Kim Y-M and Benovic JL (2002) Differential roles of arrestin-2 interaction with clathrin and adaptor protein 2 in G protein-coupled receptor trafficking. *J Biol Chem* **277**:30760–30768.
- Krasel C, Bünemann M, Lorenz K, and Lohse MJ (2005) β-arrestin binding to the β<sub>2</sub>-adrenergic receptor requires both receptor phosphorylation and receptor activation. *J Biol Chem* **280**:9528–9535.
- Krasel C, Dammeier S, Winstel R, Brockmann J, Mischak H, and Lohse MJ (2001) Phosphorylation of GRK2 by protein kinase C abolishes its inhibition by calmodulin. *J Biol Chem* **276**:1911–1915.
- Krasel C, Zabel U, Lorenz K, Reiner S, Al-Sabah S, and Lohse MJ (2008) Dual role of the β<sub>2</sub>-adrenergic receptor C terminus for the binding of β-arrestin and receptor internalization. *J Biol Chem* **283**:31840–31848.
- Lanzerstorfer P, Borgmann D, Schütz G, Winkler SM, Höglinger O, and Weghuber J (2014) Quantification and kinetic analysis of Grb2-EGFR interaction on micro-patterned surfaces for the characterization of EGFR-modulating substances. *PLoS ONE* **9**:e92151.
- Lohse MJ, Andexinger S, Pitcher J, Trukawinski S, Codina J, Faure JP, Caron MG, and Lefkowitz RJ (1992) Receptor-specific desensitization with purified proteins. Kinase dependence and receptor specificity of β-arrestin and arrestin in the β<sub>2</sub>-adrenergic receptor and rhodopsin systems. *J Biol Chem* **267**:8558–8564.
- Lutz S, Freichel-Blomquist A, Yang Y, Rümennapp U, Jakobs KH, Schmidt M, and Wieland T (2005) The guanine nucleotide exchange factor p63RhoGEF, a specific link between G<sub>q/11</sub>-coupled receptor signaling and RhoA. *J Biol Chem* **280**:11134–11139.
- Nobles KN, Xiao K, Ahn S, Shukla AK, Lam CM, Rajagopal S, Strachan RT, Huang T-Y, Bressler EA, and Hara MR et al. (2011) Distinct phosphorylation sites on the β<sub>2</sub>-adrenergic receptor establish a barcode that encodes differential functions of β-arrestin. *Sci Signal* **4**:ra51.
- Oakley RH, Laporte SA, Holt JA, Barak LS, and Caron MG (1999) Association of β-arrestin with G protein-coupled receptors during clathrin-mediated endocytosis dictates the profile of receptor resensitization. *J Biol Chem* **274**:32248–32257.
- Oakley RH, Laporte SA, Holt JA, Barak LS, and Caron MG (2001) Molecular determinants underlying the formation of stable intracellular G protein-coupled receptor-β-arrestin complexes after receptor endocytosis. *J Biol Chem* **276**:19452–19460.
- Oakley RH, Laporte SA, Holt JA, Caron MG, and Barak LS (2000) Differential affinities of visual arrestin, β arrestin1, and β arrestin2 for G protein-coupled receptors delineate two major classes of receptors. *J Biol Chem* **275**:17201–17210.
- Pal K, Mathur M, Kumar P, and DeFea K (2013) Divergent β-arrestin-dependent signaling events are dependent upon sequences within G-protein-coupled receptor C termini. *J Biol Chem* **288**:3265–3274.
- Pitcher JA, Freedman NJ, and Lefkowitz RJ (1998) G protein-coupled receptor kinases. *Annu Rev Biochem* **67**:653–692.
- Ren X-R, Reiter E, Ahn S, Kim J, Chen W, and Lefkowitz RJ (2005) Different G protein-coupled receptor kinases govern G protein and β-arrestin-mediated signaling of V2 vasopressin receptor. *Proc Natl Acad Sci USA* **102**:1448–1453.
- Seibold A, January BG, Friedman J, Hipkin RW, and Clark RB (1998) Desensitization of β<sub>2</sub>-adrenergic receptors with mutations of the proposed G protein-coupled receptor kinase phosphorylation sites. *J Biol Chem* **273**:7637–7642.
- Seibold A, Williams B, Huang Z-F, Friedman J, Moore RH, Knoll BJ, and Clark RB (2000) Localization of the sites mediating desensitization of the β<sub>2</sub>-adrenergic receptor by the GRK pathway. *Mol Pharmacol* **58**:1162–1173.
- Stenmark H, Aasland R, Toh BH, and D'Arrigo A (1996) Endosomal localization of the autoantigen EEA1 is mediated by a zinc-binding FYVE finger. *J Biol Chem* **271**:24048–24054.
- Tobin AB, Butcher AJ, and Kong KC (2008) Location, location, location...site-specific GPCR phosphorylation offers a mechanism for cell-type-specific signalling. *Trends Pharmacol Sci* **29**:413–420.
- Tohgo A, Choy EW, Gesty-Palmer D, Pierce KL, Laporte S, Oakley RH, Caron MG, Lefkowitz RJ, and Luttrell LM (2003) The stability of the G protein-coupled receptor-β-arrestin interaction determines the mechanism and functional consequence of ERK activation. *J Biol Chem* **278**:6258–6267.
- Vaughan DJ, Millman EE, Godines V, Friedman J, Tran TM, Dai W, Knoll BJ, Clark RB, and Moore RH (2006) Role of the G protein-coupled receptor kinase site serine cluster in β<sub>2</sub>-adrenergic receptor internalization, desensitization, and β-arrestin translocation. *J Biol Chem* **281**:7684–7692.
- Vishnivetskiy SA, Raman D, Wei J, Kennedy MJ, Hurley JB, and Gurevich VV (2007) Regulation of arrestin binding by rhodopsin phosphorylation level. *J Biol Chem* **282**:32075–32083.
- Wolters V, Krasel C, Brockmann J, and Bünemann M (2015) Influence of G<sub>αq</sub> on the dynamics of m3-acetylcholine receptor-g-protein-coupled receptor kinase 2 interaction. *Mol Pharmacol* **87**:9–17.
- Zidar DA, Violin JD, Whalen EJ, and Lefkowitz RJ (2009) Selective engagement of G protein coupled receptor kinases (GRKs) encodes distinct functions of biased ligands. *Proc Natl Acad Sci USA* **106**:9649–9654.

---

**Address correspondence to:** Cornelius Krasel, Institut für Pharmakologie und Klinische Pharmazie, Karl-von-Frisch-Str. 1, 35043 Marburg, Germany. E-mail: cornelius.krasel@staff.uni-marburg.de

---